Fast Parallel Direct Solvers for Coarse Grid Problems

H. M. Tufo
P. F. Fischer*

Abstract

We develop a fast direct solver for parallel solution of "coarse grid" problems, $A\underline{x} = \underline{b}$, such as arise when domain decomposition or multigrid methods are applied to elliptic partial differential equations in d space dimensions. The approach is based on a (quasi-) sparse factorization of the *inverse* of A. If A is $n \times n$ and the number of processors is P, our approach requires $O(n^\gamma \log_2 P)$ time for communication and $O(n^{1+\gamma}/P)$ time for computation, where $\gamma \equiv \frac{d-1}{d}$. Results from a 512-node Intel Paragon show that our algorithm compares favorably with more commonly used approaches that require $O(n \log_2 P)$ time for communication and $O(n^{1+\gamma})$ or $O(n^2/P)$ time for computation. Moreover, for leading-edge multicomputer systems with thousands of processors and $n = P$ (i.e., communication-dominated solves), we expect our algorithm to be markedly superior because it achieves substantially reduced message volume and arithmetic complexity over competing methods while retaining minimal message startup cost.

*Mathematics and Computer Science Division, Argonne National Laboratory, Argonne, IL 60439, USA. E-mail: *tufo@mcs.anl.gov*, *fischer@mcs.anl.gov*

1 Introduction

In this paper we consider direct solution methods for linear systems of the form

$$A\underline{x} = \underline{b}\,, \tag{1}$$

where A is an $n \times n$ sparse symmetric positive definite (SPD) matrix, such as arise from finite difference or finite element discretizations of d-dimensional elliptic partial differential equations (PDEs). We target our algorithm for the "fine-grained" regime (i.e., $n/P \approx 1$) and large numbers of processors, P. Such fine-grained solvers are required for the solution of the coarse grid systems encountered when using multigrid or domain decomposition methods to solve larger linear systems (e.g., [3, 4]). This work focuses on the coarse grid *solution* times rather than factor times, as we expect to amortize the factorization costs over several iterations and/or time-steps of the larger governing systems. Per force, the coarse grid data and solution before and after the solve stage are distributed, so it is not possible to consider solving the problem on fewer processors (artificially increasing n/P) without inducing additional communication overhead.

The problem of the coarse grid solve has been studied widely in the domain decomposition community. Widlund [16] established that order-independent convergence rates in domain decomposition methods cannot be obtained without the solution of a coarse grid problem. In [3], Chan and Shao present a study of the optimal coarse grid size for parallel applications that illustrates the importance of a fast coarse grid solver. Gropp et al. [9, 11, 14] also discuss the importance and challenge of developing an efficient parallel coarse grid solver for domain decomposition methods. Cai [2] has developed a domain decomposition scheme requiring a very low dimensional coarse grid space where much of the information transfer is through the action of the restriction/prolongation operators. Nonetheless, it is clear that a multicomputer implementation of the coarse grid problem must require communication in the prolongation/restriction phase or have a minimum of one degree of freedom per processor, that is, $n \geq P$.

Since leading-edge multicomputer systems are currently scaling to thousands of processors, there is a clear need for an efficient treatment of the parallel coarse grid problem. In particular, if the work per processor remains constant while the number of processors increases (the standard model for scaled speedup [12]), the coarse grid problem will ultimately dominate the complexity unless the solve time can be substantially reduced.

In this paper we discuss a fast parallel coarse grid solution algorithm based on creating a sparse A-conjugate basis for $\mathbb{R}^n$ to be denoted by the columns of the matrix

$$X = (\underline{x}_1, \ldots, \underline{x}_n)\,.$$

We show that this approach constitutes a sparse factorization (not necessarily triangular) of the full matrix A^{-1}. The scheme has a per-solve complexity of $O(n^\gamma \log_2 P)$ for communication and $O(n^{1+\gamma}/P)$ for computation, where $\gamma \equiv \frac{d-1}{d}$. This compares quite favorably with more commonly used approaches that require $O(n \log_2 P)$ time for communication and $O(n^{1+\gamma})$ or $O(n^2/P)$ time for computation. Results obtained on a 512-node Intel Paragon

show that our method performs well even for values of n/P significantly greater than unity, particularly for larger values of P.

The outline of the paper is as follows. Section 2 briefly describes several communication primitives central to distributed direct solution methods. Section 3 reviews several existing coarse grid solution strategies. Section 4 discusses the computational and communication complexity for the present approach. In Section 5 we present performance results for a $\sqrt{n} \times \sqrt{n}$ grid problem on a 512-node Intel Paragon. Finally, current research efforts, possible extensions of the algorithm, and expected performance on thousands of processors are presented in Section 6.

2 Communication Primitives

In this section, we review the communication complexity of several all-to-all communication schemes of relevance to coarse grid solvers.

If the originating PDE has an elliptic component, the inverse of A will be a full matrix. Consequently, the computation of

$$\underline{x} = A^{-1}\underline{b} \tag{2}$$

for distributed vectors $\underline{x}$ and $\underline{b}$ will require some type of all-to-all communication; any nonzero element of $\underline{b}$ will influence every element of $\underline{x}$. By definition, coarse grid problems are relatively fine grained, implying that communication accounts for a substantial fraction of the solution time. Moreover, the messages often are quite short, implying that the communication phase is latency dominated; hence, minimizing the total number of message startups is of paramount importance. If we assume that the compute nodes can receive only one message at a time, it follows that the minimum number of message cycles required to effect the requisite all-to-all communication in the evaluation of (2) is $\log_2 P$; we take this as a lower bound on the solution time.

We assume a standard linear model for contention-free interprocessor communication in which the time to send an m-word message is given by

$$t_c[m] = (\alpha + \beta m)t_a \,, \tag{3}$$

where α is the message startup cost (latency), β is the asymptotic per-word-transfer cost (inverse bandwidth), and t_a is the characteristic time for an arithmetic operation. Typically, $\alpha \gg \beta \gg 1$. Thus, optimal communication strategies may possibly require a balance between minimizing the number of messages and the length (m) of the messages. We assume that contention-free transit time is independent of the distance between processors (i.e., the processor network can be modeled as a switching network).

Our communication analysis in the forthcoming sections will be based on the use of fan-in/fan-out reduction operations, which are guaranteed to be contention-free, even on one-dimensional networks. To clarify this point, consider the implementation of two common reduction operations, vector concatenation and vector summation. The first gathers a distributed m-vector having $m_p = m/P$ components on each processor, $p = 0, 1, \ldots, P-1$.

The second computes

$$\underline{v} = \sum_{p=0}^{P-1} \underline{v}^{(p)} ,$$

where each $\underline{v}^{(p)}$ is an m-vector. Assuming $P = 2^D$, these algorithms can be described as follows:

Procedure Vector-Concatenate

Gather via binary fan-in

```
   m̂ := m_p
   do l = 1 to D
      if mod(p, 2^l) = 0 then
         recv v(m̂+1:2m̂) from p + 2^(l-1)
      else
         send v(1:m̂) to p - 2^(l-1)
         goto 1
      endif
      m̂ := 2m̂
   enddo
```

Broadcast via binary fan-out

```
1  do l = D to 1 by -1
      if mod(p, 2^l) = 0 then
         send v(1:m) to p + 2^(l-1)
      elseif mod(p, 2^(l-1)) = 0 then
         recv v(1:m) from p - 2^(l-1)
      endif
   enddo
```

Procedure Vector-Sum

Gather via binary fan-in

```
   do l = 1 to D
      if mod(p, 2^l) = 0 then
         recv w(1:m) from p + 2^(l-1)
         v(1:m) := v(1:m) + w(1:m)
      else
         send v(1:m) to p - 2^(l-1)
         goto 1
      endif
   enddo
```

Broadcast via binary fan-out

```
1  do l = D to 1 by -1
      if mod(p, 2^l) = 0 then
         send v(1:m) to p + 2^(l-1)
      elseif mod(p, 2^(l-1)) = 0 then
         recv v(1:m) from p - 2^(l-1)
      endif
   enddo
```

In the fan-in stage, communication begins between neighboring processors, then neighbors of neighbors, and so forth, until in the last stage processor P/2 sends data to processor 0. In the case that the processors are ordered sequentially along a one-dimensional network or that $P = 2^D$ processors in a two-dimensional grid are labeled using a standard lexicographical ordering, there is no contention for communication links as the distance between processors increases because the intermediary processors become inactive once they have sent data. The concatenate routine requires $(\alpha \log_2 P + \beta \cdot (m - m_p))t_a$ time for the gather, plus an additional $(\alpha + \beta m) \log_2 P \, t_a$ time for the broadcast, for a total time of approximately $(2\alpha + \beta m) \log_2 P \, t_a$. The vector sum requires a total time of $(2\alpha + 2\beta m + m) \log_2 P \, t_a$, with the extra $m \log_2 P t_a$ term accounting for the vector summation in line four of the algorithm.

In contrast to the fan-in/fan-out strategy the respective operations can also be implemented via recursive doubling as follows:

Procedure Vector-Concatenate
Recursive Doubling
$\hat{m} := m_p$
do $l = 1$ to D
  send $v(1:\hat{m})$ to $mod\,(p + 2^{l-1}, P)$
  recv $v(\hat{m}+1:2\hat{m})$ from $mod\,(P+p-2^{l-1}, P)$
  $\hat{m} := 2\hat{m}$
enddo

Procedure Vector-Sum
Recursive Doubling
do $l = 1$ to D
  send $v(1:m)$ to $mod\,(p + 2^{l-1}, P)$
  recv $w(1:m)$ from $mod\,(P+p-2^{l-1}, P)$
  $v(1:m) := v(1:m) + w(1:m)$
enddo

In this case, the concatenate routine nominally requires time $(\alpha \log_2 P + \beta \cdot (m - m_p))t_a$, roughly a factor of $\log_2 P$ better than the fan-in/fan-out approach. The vector sum routine requires a nominal time of $(\alpha + \beta m + m)\log_2 P\, t_a$, roughly a factor of two superior to the fan-in/fan-out approach. On hypercubes, the recursive doubling algorithms can be implemented with a contention-free schedule. However, on low-dimensional networks the recursive doubling schemes will suffer observable network link contention unless the problem is latency dominated, i.e., $m \lesssim \alpha/\beta$. Consequently, the performance will generally be inferior to the fan-in/fan-out approach.

It is worth noting that hybrid approaches are possible. For example, for concatenation, recursive doubling can be used until $\hat{m} \approx \alpha/\beta$ and fan-in/fan-out then used on processor subsets to span the remaining levels of the tree(s). For vector summation there is a well-known hybrid scheme due to van de Geijn et al. [15] that is effective when $m \gg \alpha/\beta$. For the values of m required for the coarse grid solution schemes considered here, the fan-in/fan-out schemes capture the essential complexity, while hybrid schemes would be most appropriate as a fine-tuning measure in the final implementation phases, so we do not consider them further.

To put the forthcoming discussion of solution strategies on a firm foundation, we briefly review the communication requirements of a typical matrix-vector multiplication implementation on $P = 2^D$ processors. Assume $\underline{x}$ is a vector having n components, $(x_1, \ldots, x_{i_g}, \ldots, x_n)$, which are distributed across P processors according to the bijective map, $i_g = \mu(i,p) \in \{1, \ldots, n\}$, where $i \in \{1, \ldots, n_p\}$ is the local index on processor p, for $p \in \{0, \ldots, P-1\}$. The global-to-local mapping is specified by the inverse mapping, $(i,p) = \mu^{-1}(i_g)$. We assume, without loss of generality, that the number of components of $\underline{x}$ on each processor p is the same, namely, $n_p = n/P$. Let $C = (\underline{c}_1\, \underline{c}_2 \ldots \underline{c}_n)$ be an $n \times n$ matrix with each column, $\underline{c}_i$, partitioned according to the same distribution as $\underline{x}$ (i.e., *rows* of C are contiguous within a processor, with row $\mu(i,p)$ of C mapped to row i on processor p). Then $\underline{y} = C\underline{x}$ is computed as follows. First, a copy of $\underline{x}$ is gathered onto each processor using a vector-concatenate procedure. Then, each processor p computes the inner-products $y_{\mu(i,p)} = \underline{x}^T \underline{r}_{\mu(i,p)}$ for $i = 1, \ldots, n_p$, where $\underline{r}_\mu$ is the μth row of C. The end result is a vector $\underline{y}$ that is distributed according to the mapping μ. If C is full, the matrix-vector product complexity is $2n \cdot n_p t_a = 2(n^2/P)t_a$ for the local inner-products plus $(2\alpha + \beta m)\log_2 P\, t_a$ for the gather. We remark that the DAXPY-based approach in which the communication is performed after the computation can be implemented with identical complexity if one chooses to store C in a column-contiguous format.

3 Survey of Coarse Grid Solvers

It is well known (e.g., [9]) that parallel solution of the coarse grid problem is hampered by the inherent sequentiality of the forward and backward substitution phases of standard triangular (LU or LL^T) solves. If n (and, consequently, P) is sufficiently small, it is feasible to store, factor, and solve the system locally within a single processor, thus allowing the use of standard serial solvers. On a low-dimensional network, the optimal variant of this scheme is to concatenate $\underline{b}$ via the binary fan-in scheme of the preceding section, solve the problem on the root, and then cascade the solution from the root using the inverse of the concatenation procedure. If the local solution strategy is based on banded solvers, the computational complexity is $4ns$ operations for a matrix of bandwidth s, while the communication complexity is $2\alpha \log_2 P + 2\beta n$, as noted in the preceding section. For historical reasons, it is more common to solve the problem redundantly on each processor, obviating the need to broadcast the solution. On a hypercube, such a strategy is sensible because the recursive doubling variant of concatenation is contention free and the communication cost is halved. However, on lower-dimensional networks, the optimal communication strategy for the redundant solution approach is based on fan-in/fan-out, with a cost of $(2\alpha + \beta n) \log_2 P \, t_a$.

For large numbers of processors and relatively small systems (e.g., $P > 128$, $n < 5000$), computing the full inverse of A can be far more effective than solving the system redundantly (e.g., [6, 10]). By distributing the rows of A^{-1} in the same manner as $\underline{x}$ and $\underline{b}$, the solution can be computed as a parallel matrix-vector product, $A^{-1}\underline{b}$, once $\underline{b}$ has been gathered onto each processor. The communication complexity is identical to that of the redundant LU method described above; however, the complexity for the computation of the inner-products of the rows of A^{-1} with $\underline{b}$ is $2n^2/P$. Parallelism has been introduced to this phase of the solution, and it follows that the distributed A^{-1} approach is superior whenever $P > \frac{n}{2s}$.

The advantage of the distributed A^{-1} method is that matrix-vector multiplication is intrinsically parallel. Unfortunately, A^{-1} is completely full, and, consequently, the storage cost of n^2/P per processor limits this approach to values of n of up to only a few thousand in practice. With the advent of computers containing thousands of processors, this restriction is problematic. Ideally, one would like a matrix-vector product-based approach involving *sparse* matrices.

A step in this direction is the method of Alvarado et al. [1] who develop fast parallel triangular solvers by recasting the inverse of a sparse triangular matrix, L, as a product of l sparse factors, $\tilde{L}_i^{-1}$, each of which can be computed in place. The solution for a single triangular system is then given by the sequence of products $\underline{v}_0 = \underline{b}$, $\underline{v}_i = \tilde{L}_i^{-1}\underline{v}_{i-1}, \ldots, \underline{x} = \tilde{L}_l^{-1}\underline{v}_{l-1}$. Analysis of this approach is quite difficult, since each factor is sparse, and it's unclear where data is located at the start and finish of each multiplication. However, Alvarado et al. strive to minimize l, in which case each matrix-vector product must be performed in turn, with communication taking place in between (otherwise, there would be further parallelism to be exploited, and l would therefore not be minimal). Assuming that the work of each matrix-vector product is distributed across P processors, we estimate the communication time for each of the l cycles as $t_c = 2\alpha(\log_2 P)t_a$. If A is the discrete Laplacian for a problem on a two-dimensional grid, the number of factors is typically $l \approx$

$\log_2 \sqrt{n} \approx \log_2 \sqrt{P}$ (see, e.g., [8]). Since solution of (**??**) requires both a forward and backward sweep, we estimate a lower bound on the solution time of $2\alpha(\log_2 P)^2 t_a$. This estimate neglects both the work, which, with a lower bound of $\Omega(\frac{n \log_2 n}{P})$ [8], probably is negligible, and the amount of data communicated, which probably is not negligible.

Another approach of interest is that of Farhat and Chen [5], who solve the coarse grid problem by projecting onto sets of previously generated Krylov vectors that constitute an approximation space. Let $X_k = (\underline{x}_1 \ \underline{x}_2 \ \ldots \ \underline{x}_k)$ be a matrix of A-conjugate vectors normalized to satisfy

$$\underline{x}_i^T A \underline{x}_j \ = \ \delta_{ij} \,, \tag{4}$$

where δ_{ij} is the Kronecker delta. Then

$$\bar{\underline{x}} = X_k X_k^T \underline{b} \tag{5}$$

yields the projection onto $\mathcal{R}(X_k)$ satisfying

$$\bar{\underline{x}} \in \mathcal{R}(X_k) \,, \qquad ||\underline{x} - \bar{\underline{x}}||_A \leq ||\underline{x} - \underline{v}||_A \quad , \quad \forall \underline{v} \in \mathcal{R}(X_k) \,. \tag{6}$$

Here, $\mathcal{R}(\cdot)$ denotes the range of the argument, and $||\cdot||_A$ denotes the A-norm given by $||\underline{w}||_A = (\underline{w}^T A \underline{w})^{\frac{1}{2}}$.

Farhat and Chen build the space $\mathcal{R}(X_k)$ by collecting the A-conjugate search directions generated in the course of applying (a slightly modified) conjugate gradient (CG) iteration to (1) for several right-hand sides. In time transient problems, the successive right-hand sides often share enough information such that very few CG iterations are required to solve the problem subsequent to the initial projection (6). In the examples reported in [5], Farhat and Chen observe that superconvergence sets in for $k \gtrsim 0.25n$, at which point only one or two conjugate gradient iterations are required subsequent to the initial projection.

We can estimate the complexity of the projection+CG approach by computing the cost of the projection step (though the subsequent CG iteration cost is in fact non-negligible). Assume that each basis vector, $\underline{x}_j$, is distributed in the same fashion as $\underline{x}$ and $\underline{b}$. To compute $\bar{\underline{x}} = X_k X_k^T \underline{b}$, one first computes an intermediate k-vector, $\underline{c} = X^T \underline{b}$, in two stages, beginning with evaluation of the local dot products

$$c_j^{(p)} \quad = \quad \sum_{i=1}^{n_p} b_{\mu(i,p)} \, x_{\mu(i,p),j} \,, \qquad \begin{array}{l} j \in 1, \ldots, k \\ p \in 0, \ldots, P-1 \,, \end{array} \tag{7}$$

followed by a $\log_2 P$ sum across processors

$$c_j \quad = \quad \sum_{p=0}^{P-1} c_j^{(p)} \qquad j \in 1, \ldots, k \,. \tag{8}$$

With the components of $\underline{c}$ known to every processor, the distributed vector $\bar{\underline{x}}$ is computed as

$$\bar{x}_{\mu(i,p)} \quad = \quad \sum_{j=1}^{k} c_j x_{\mu(i,p),j} \qquad \begin{array}{l} i \in 1, \ldots, n_p \\ p \in 0, \ldots, P-1 \,. \end{array} \tag{9}$$

This final stage is recognized as a sequence of k DAXPYs, $\underline{\bar{x}}^{(p)} = \underline{\bar{x}}^{(p)} + c_j \underline{x}_j^{(p)}$, of length n_p on each processor p, and is fully concurrent.

If the vectors $\underline{x}_j$ are full, this approximation has leading-order computational complexity of $4nk/P$ operations for the required dot products (7) and DAXPYs (9). The communication time for the gather of the k coefficients of each column vector (8) is $\log_2 P(2\alpha + 2\beta k + k)t_a$, where the last k term accounts for the summation in (8). Note that if $k = O(n)$, then the projection approach is better than the distributed A^{-1} approach by at most a constant, with a lower bound solution time of $2\alpha t_a \log_2 P$ being obtained for both methods. Furthermore, any CG iterations required for the projection+CG scheme will incur additional latency overhead of at least $2\alpha t_a \log_2 P$ per iteration due to the inner-products required for the CG algorithm.

In the next section, we present a projection method for which $k \equiv n$ but which, by virtue of using a *sparse* basis set, X, achieves communication and computation complexities that are of lower order than the A^{-1} approach. Moreover, this approach requires a minimum number of message cycles and thus achieves the lower bound latency time of $2\alpha t_a \log_2 P$.

4 Sparse Basis Projection Method

The goal of the method of Farhat and Chen [5] is to choose a basis set X_k such that $\underline{\bar{x}}$ is a good approximation to $\underline{x}$. We observe that if $k = n$, then $\mathcal{R}(X_k) = \mathbb{R}^n$ and, from (6), $\underline{\bar{x}} \equiv \underline{x}$. This implies that $X_n X_n^T$ is the inverse of A. In [7], we introduced a method in which the projection approach is modified to incorporate a matrix of n basis vectors, $X \equiv X_n$, which is as sparse as possible and which yields significantly reduced computational and communication complexities. We now describe the implementation of the method and discuss communication considerations in depth. In the next section, we consider the implementation of the XX^T based method for a $\sqrt{n} \times \sqrt{n}$ model problem on the 512-node Intel Paragon and compare its performance with that of the redundant LU and A^{-1} approaches of Section 3.

4.1 Basis

We begin with the following observation. Let the unit vectors $\underline{\hat{e}}_i$ and $\underline{\hat{e}}_j$ denote the ith and jth column of the $n \times n$ identity matrix. Let $\mathcal{N}_j$, the *neighborhood* of j, be the set of row indices corresponding to nonzeros in column j of A, that is, $i \in \mathcal{N}_j$ *iff* $a_{ij} \neq 0$. Then

$$\underline{\hat{e}}_i^T A \underline{\hat{e}}_j \quad = \quad 0 \qquad \forall\, i \notin \mathcal{N}_j \quad .$$

Geometrically, this corresponds to the situation for the 9-point stencil shown in Fig. 1a. (In this and subsequent figures, the degrees of freedom are associated with the centroids of the cells in the computational grid.) From this figure it is clear that at least $n/\max(\#\mathcal{N}_j)$ of the unit vectors are A-conjugate to one another, where $\#\mathcal{N}_j$ is the cardinality of $\mathcal{N}_j$.

The generation of a sparse basis for X starts with finding a maximal (or near-maximal) set of k_1 A-conjugate unit vectors and normalizing them to satisfy (4). The first such k_1 columns of X will each have *only one nonzero entry.* Additional entries in X are generated

via Gram-Schmidt orthogonalization. Let $X_k = (X_{k-1}\ \underline{x}_k)$ denote the $n \times k$ matrix with columns $(\underline{x}_1\ \underline{x}_2 \ldots \underline{x}_k)$, and let $V = (\underline{v}_1\ \underline{v}_2 \ldots \underline{v}_n)$ be an appropriate permutation of the identity matrix. Then the procedure

$$
\begin{aligned}
&do\ \ k = 1, \ldots, n\text{:} \\
&\quad \underline{w} := \underline{v}_k \ - \ X_{k-1} X_{k-1}^T A \underline{v}_k \qquad (10) \\
&\quad \underline{x}_k := \underline{w} / ||\underline{w}||_A \\
&\quad X_k := (X_{k-1}\ \underline{x}_k) \\
&enddo
\end{aligned}
$$

ensures that $X = X_n$ is the desired factor of A^{-1}. For $k \leq k_1$ the projection, $X_{k-1} X_{k-1}^T A \underline{v}_k$, computed in (10) will be void and $\underline{x}_k$ will simply be a multiple of $\underline{v}_k$. As k increases beyond k_1, X_k will begin to fill in. The goal is to find an ordering, V, which yields minimal or near minimal fill for the factor X.

Following [8], an efficient procedure for selecting the permutation matrix, V, can be developed by defining separators that recursively divide the domain (or graph) associated with A into nearly equal subdomains. For a $\sqrt{n} \times \sqrt{n}$ grid the first such separator is shown in Fig. 1b. Since the stencil for $A\hat{\underline{e}}_j$ does not cross the separator, it is clear that every unit vector $\hat{\underline{e}}_i$ associated with the left half of the domain in Fig. 1b is A-conjugate to every unit

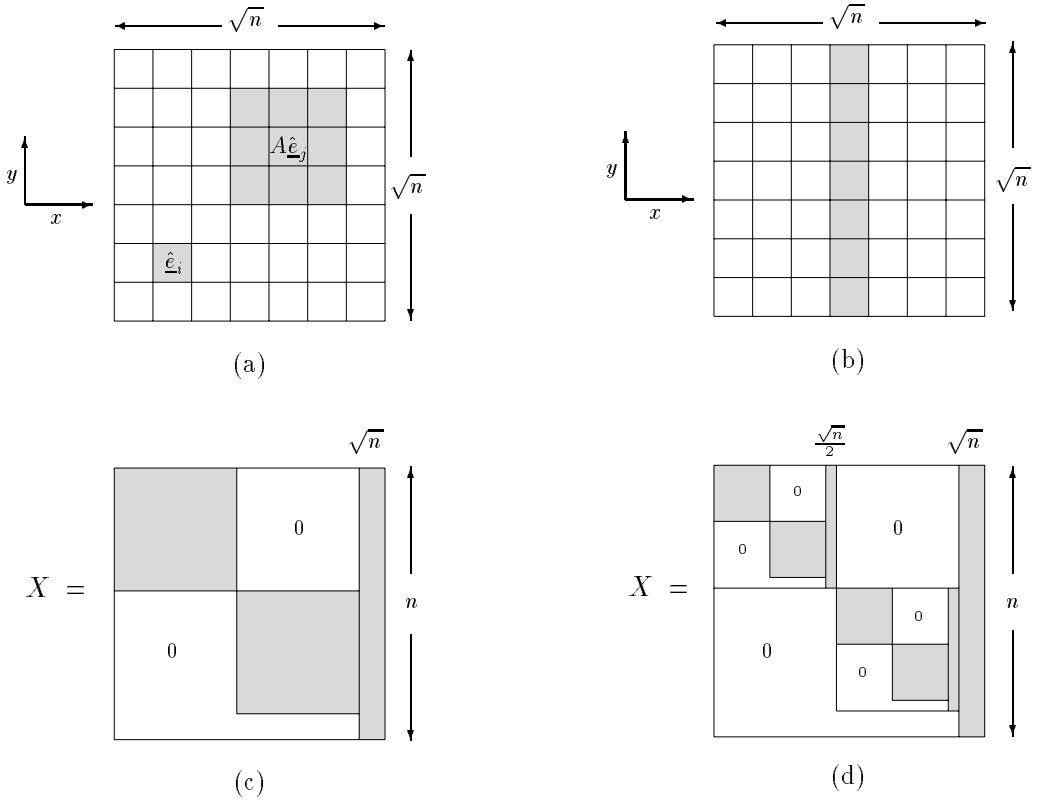

Figure 1: (a) geometric support (shaded) of orthogonal vectors $\hat{\underline{e}}_j$ and $A\hat{\underline{e}}_i$, (b) support of separator set, (c) zero/fill structure for X resulting from ordering the separator set last, (d) zero/fill structure after second round of recursion.

vector $\hat{\underline{e}}_j$ associated with the right half. If V is arranged such that vectors associated with the left half of the domain are ordered first, vectors associated with the right half second, and vectors associated with separator last, then application of Gram-Schmidt orthogonalization will generate a matrix X with worst-case fill depicted by Fig. 1c (X is shown here with the rows reordered according to the permutation used for the columns of V). This procedure can be repeated to order the vectors within each subdomain, giving rise to the structure shown in Fig. 1d. To complete the construction, we recur until no more separators can be found.

It is clear from (5) that the computational complexity of each solve is proportional to the amount of nonzero fill in the factor X. For the $\sqrt{n} \times \sqrt{n}$ grid we observe from Fig. 1d that the number of nonzeros in each row is bounded by the sequence

$$\sqrt{n} + \frac{\sqrt{n}}{2} + \frac{\sqrt{n}}{2} + \frac{\sqrt{n}}{4} + \frac{\sqrt{n}}{4} + \ldots \leq 3\sqrt{n}\,,$$

implying a total bound on the amount of fill in X of $3n\sqrt{n}$. Since we can evenly distribute the work among processors, we get a computational complexity of $O(n^{\frac{3}{2}}/P)$. Similar arguments in three-dimensions lead to a computational complexity of $O(n^{\frac{5}{3}}/P)$. Both the two and three-dimensional cases provide a clear gain over the $O(n^2/P)$ cost incurred by the full inverse approach.

The communication complexity is dependent on the mapping of the rows of X (and hence, $\underline{x}$ and $\underline{b}$) to the processors. In the worst case, the bound is simply that derived for (8), namely, $\log_2 P(2\alpha + 2\beta n + n)t_a$, which is essentially the same as the A^{-1} approach. Because of the significant reduction in computational complexity, even a naive implementation of the XX^T approach will be superior to the A^{-1} approach. However, for properly mapped two-dimensional problems, it is possible to obtain a contention-free communication complexity bound of $(2\alpha \log_2 P + O(n^{\frac{1}{2}})\beta \log_2 P)t_a$, even on a linear array of processors. The three-dimensional bound has the form $(2\alpha \log_2 P + O(n^{\frac{2}{3}})\beta \log_2 P)t_a$. Results in Section 5 show that, for large problems, this lower communication complexity is as significant as the improved computational complexity in reducing the overall solution time.

4.2 A Detailed Example

To understand the ordering and processor mapping requirements necessary to reduce the communication complexity, we consider the 7×7 grid example of Fig. 2 in some detail. As in Fig. 1, the degrees of freedom are represented by the square cells shown in (a), and it is assumed that A has a 3×3 stencil. The first three levels of separators have been labeled in (a), and an associated hierarchy is depicted by the binary tree in (b). To obtain the desired nonzero structure of X, the separator labeling is continued until all degrees of freedom have been identified as an element of a separator. The degrees of freedom are then labeled in reverse order, $i = n, \ldots, 1$, using a depth-first traversal of the tree. One begins with elements in separator S_0, followed by those in S_2, S_{22}, and so on, to yield the orderings shown in (c) and (d). The descendants of an element j are denoted as the set D_j comprising j and any element i that is below j in the tree.

The Gram-Schmidt procedure (10) does not require the rows of X to be permuted with the same ordering as the columns. However, there are notational and implementation advantages to doing so. Thus, from here on we assume that A has been constructed according to the ordering in Fig. 2c, corresponding to a symmetric permutation of the original operator. In this case, the Gram-Schmidt procedure (10) is simplified in that the basis vectors become $\underline{v}_k = \underline{\hat{e}}_k$, $k = 1, \ldots, n$. Because of the reversed depth-first ordering, this corresponds to starting at the leaves of the tree (not shown in Fig. 2d); subsequent unit vectors are selected for orthogonalization only after their descendants. By construction, a unit vector $\underline{\hat{e}}_k$ is automatically A-conjugate to any unit vector which is not its direct descendant or direct ancestor. Hence, the Gram-Schmidt projection step only needs to be effected against the columns of X_{k-1} that correspond to descendants of k. Thus, (10) is

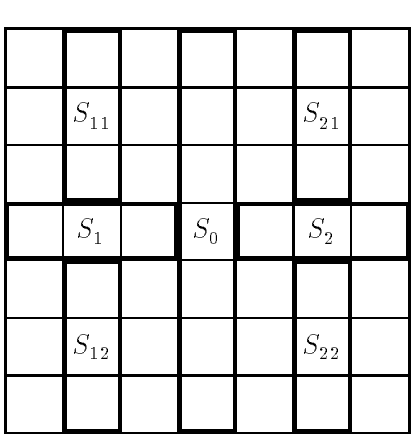

(a)

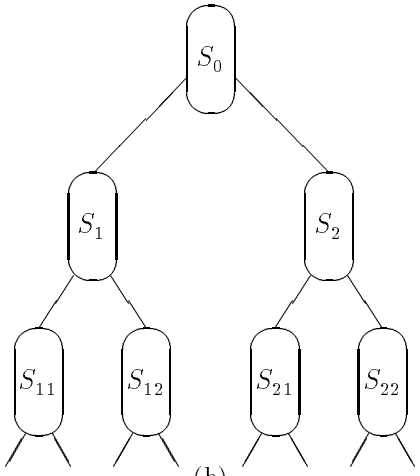

(b)

2	9	5	49	23	30	26
3	8	6	48	24	29	27
1	7	4	47	22	28	25
19	20	21	46	40	41	42
11	18	14	45	32	39	35
12	17	15	44	33	38	36
10	16	13	43	31	37	34

(c)

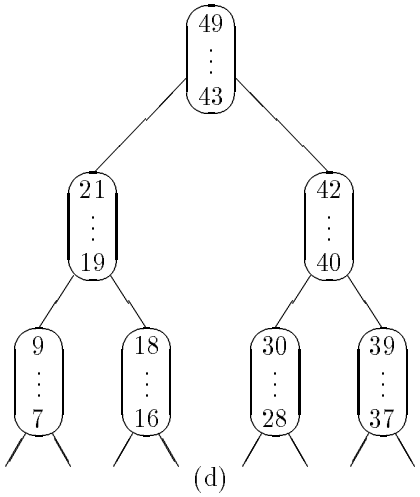

(d)

Figure 2: (a) separator sets (only first three levels shown), (b) separator set tree, (c) global numbering induced by depth first ordering of separator sets, (d) global numbering embedded in separator set tree.

recast as

$$
\begin{aligned}
&do\ \ k = 1, \ldots, n\text{:} \\
&\quad \underline{w}_k := \hat{\underline{e}}_k \ - \sum_{j \in D_k \backslash k} \underline{x}_j (\underline{x}_j^T A \hat{\underline{e}}_k) \qquad (11) \\
&\quad \underline{x}_k := \underline{w}_k / ||\underline{w}_k||_A \\
&\quad X_k := (X_{k-1}\ \underline{x}_k) \\
&enddo
\end{aligned}
$$

In general, x_{ik} will be nonzero for all elements $i \in D_k$, save the possibility of fortuitous cancellation during the projection step.

For the important case when A is an M-matrix, that is, SPD with nonpositive off-diagonal entries, then it is guaranteed that all of the entries in X are non-negative and that there will be no cancellation during the projection step (11). The non-negativity of the x_{ij}'s is established by induction. It clearly holds for the leaves of the tree because, in that case, each $\underline{x}_j$ is simply a positive multiple of $\hat{\underline{e}}_j$. Now consider the sign of the basis coefficients in the projection step (11):

$$
\begin{aligned}
c_j &= \underline{x}_j^T A \hat{\underline{e}}_k \qquad j \in \{1, ..., k-1\} \\
&= \sum_{i=1}^{n} x_{ij} a_{ik} \, . \qquad (12)
\end{aligned}
$$

Since $k > j$, we have $x_{kj} = 0$, and all terms in the summation (12) are nonpositive by the assumptions $x_{ij} \geq 0$ and $a_{ij} \leq 0$, $i \neq j$. Therefore, $c_j \leq 0$. Since the vector $c_j \underline{x}_j$ is subtracted from from $\hat{\underline{e}}_k$ in (11), all elements of $\underline{w}_k$ and hence, $\underline{x}_k$, must be positive. It is interesting to note that simply adding positive components to the unit vector $\hat{\underline{e}}_k$ yields a vector ($\underline{w}_k$) having a greater 2-norm, but reduced A-norm. We conclude that this must result from "smoothing" the Kronecker delta function represented by $\hat{\underline{e}}_k$. Indeed, for the case when A is a discrete Laplacian, plots of the element distribution on the physical mesh reveal that the basis vectors $\underline{x}_k$ (or $\underline{w}_k$) smoothly decay away from element k to the boundary of the support of D_k.

From the above arguments, we see that the number of nonzeros in any column $\underline{x}_j$ is (generally) going to be equal to $\# D_j$, that is, the number of descendants of j. It follows that the number of nonzeros in a given row, i, is given by the number of ancestors of i, that is, by counting up from the location of i to the root of the tree. For example, in Fig. 2d, the number of nonzeros in column 49 of X will be 49, whereas the number of nonzeros in row 49 will be 1. We conclude that, thus generated, X is upper triangular and therefore the unique Cholesky factor of A^{-1}.

To illustrate the significance of obtaining a proper ordering prior to generating X, we close this section with a one-dimensional example. Figures 3a and b show the sparsity patterns obtained for the upper-triangular Cholesky factor, L^T, and its inverse when A is the well-known tridiagonal matrix, $LL^T = A =$*tridiag* (-1,2,-1), deriving from a centered difference approximation to a second-order derivative. Despite the fact that L^T has the minimum possible fill, $(L^T)^{-1}$ is completely full. However, if one first permutes A using a

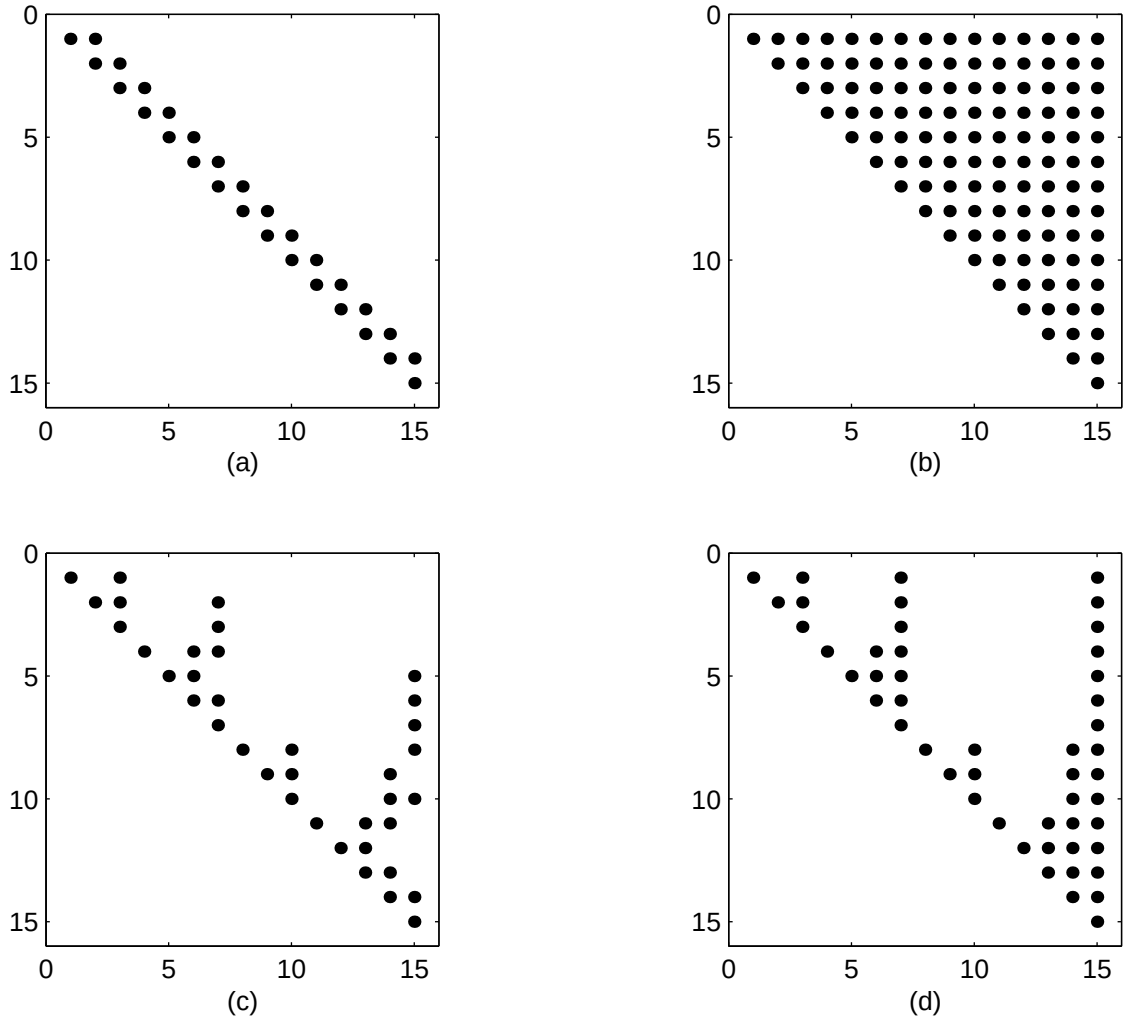

Figure 3: (a) sparsity pattern for the upper triangular Cholesky factor, L^T, of a 15×15 tridiagonal matrix, (b) sparsity pattern of $(L^T)^{-1}$, (c) sparsity pattern for the Cholesky factor, L_N^T, obtained from a nested dissection ordering of A, (d) sparsity pattern for $X = (L_N^T)^{-1}$.

depth-first nested-dissection ordering, V, and then computes the factors $L_N L_N^T = V^T A V$, one obtains the sparsity patterns shown in Figs. 3c and d. It is readily shown that in this case, the number of nonzeros in $X \equiv (L_N^T)^{-1}$ is $O(n \log n)$. Of course, because the Green's function for the associated continuous equation is nonvanishing everywhere, $XX^T = (VAV^T)^{-1}$ is completely full.

4.3 Parallel Implementation

We now examine the influence of the nonzero pattern of X on the communication requirements for the parallel solver and show that this can be exploited to obtain a communication complexity that is significantly less than $O(n)$.

Recall that the nonzeros in each column $\underline{x}_j$ correspond to descendants of j in the

separator tree, that is,

$$x_{ij} \neq 0 \implies i \in D_j .$$

Thus, the dependency graph in Fig. 2b reflects the input requirements for the evaluation of the dot products (7) and DAXPYs (9) during the computation of $XX^T\underline{b}$. The dot products, $c_j = \underline{x}_j^T \underline{b}$, are computed as

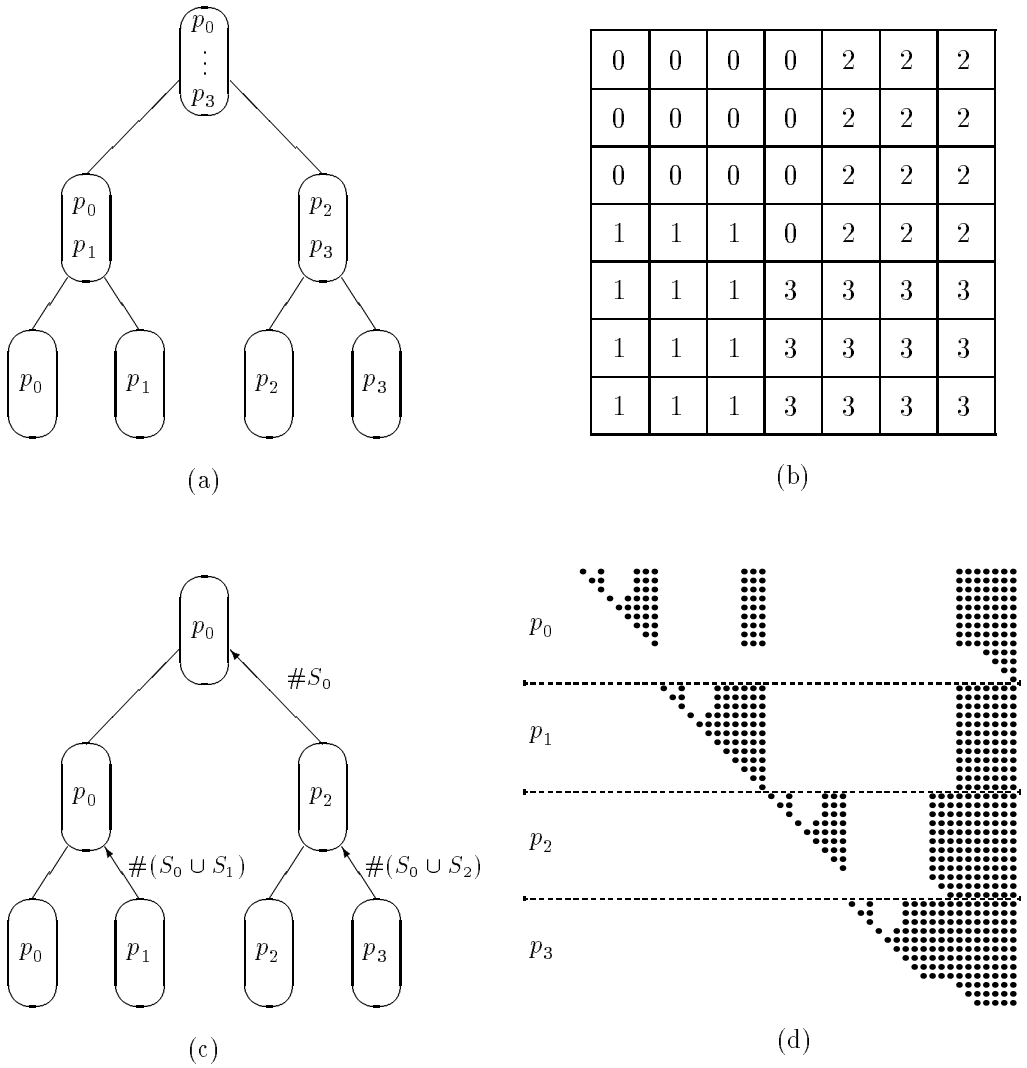

Figure 4: (a) Tree-embedding of separator-to-processor distribution for degrees-of-freedom from Fig. 2b, (b) processor mapping for degrees-of-freedom, (c) fan-in communication required during computation of $\underline{c} = X^T\underline{b}$, (d) sparsity pattern and processor distribution for X.

$$
\begin{aligned}
c_j &= \sum_{i=1}^{n} x_{ij} b_i \\
&= \sum_{x_{ij} \neq 0} x_{ij} b_i \\
&= \sum_{i \in D_j} x_{ij} b_i \,, \qquad (13)
\end{aligned}
$$

from which it is clear that the computation of c_j depends only on the descendants of j.

Communication can be minimized during the computation of c_j (13) if the lower branches of the tree are, to the extent possible, self-contained within a given processor. This can be achieved in a natural way by assigning the processor distribution during the nested dissection phase of the ordering. Degrees of freedom to the left of the first separator are assigned to the lower half-set of processors, those to the right are assigned to the upper half, and those belonging to the separator itself can be assigned to any processor in the set. Repeating this procedure recursively for the example problem of Fig. 2 leads to the element-to-processor distribution shown in Figs. 4a and b.

In general, one obtains an admissible element-to-processor map by simply overlaying the processor and separator trees. At each level, the elements of a given separator can be assigned to any processors in the pool associated with that branch of the tree. In the event that the processor tree has insufficient depth to cover the separator tree, all remaining branches in the separator tree are assigned to the associated leaves of the processor tree. In the event that the separator tree has insufficient depth to cover the processor tree, processors at the leaves would draw on elements belonging to separators above them in the tree. The latter situation will generally only arise in abstract applications. Standard domain decomposition strategies based on recursive bisection will ensure an appropriate element-to-processor map provided that separator elements are drawn from the partition boundaries generated at each bisection step.

Given a proper ordering and processor distribution, the communication for the fan-in phase (8) of the $XX^T\underline{b}$ evaluation will have the structure illustrated in Fig. 4c. The arrows indicate message sources and destinations for each of the $\log_2 P$ phases as well as the amount of data transmitted. Processors that sum incoming data are denoted in the ovals at each level of the tree. Since the evaluation of each element of $\underline{c} = X^T\underline{b}$ depends only on descendants of c_j, the amount of information that must propagate up the tree steadily decreases as the summation progress toward the root. For example, the computation of c_j, $\forall j \in S_0$ requires only $\#S_0 = \sqrt{n}$ elements to be propagated in the final phase of the fan-in.

The required communication is readily incorporated into the Vector-Sum procedure of Section 2 if the data is sorted according to the global ordering such that $\mu(i,p)$ is monotonically increasing with i for a given processor, p. Suppose that the sequence $s_l^{(p)}$, $l = 1, \ldots, D$, represents the cardinality of the separator sets encountered as one traverses from leaf p of the processor tree to the root (Fig. 4a) and that $m_p = \sum_l s_l^{(p)}$. Then the modified Vector-Sum procedure is given by

Procedure Vector-Sum 2

Gather via binary fan-in

$m_0 := 1$
do $l = 1$ to D
  if $mod\,(p, 2^l) = 0$ then
    recv $w(m_0{:}m)$ from $p + 2^{l-1}$
    $v(m_0{:}m_p) := v(m_0{:}m_p) + w(m_0{:}m_p)$
    $m_0 := m_0 + s_l^{(p)}$
  else
    send $v(m_0{:}m_p)$ to $p - 2^{l-1}$
    goto 1
  endif
enddo

Broadcast via binary fan-out

1 do $l = D$ to 1 by -1
  if $mod\,(p, 2^l) = 0$ then
    $m_0 := m_0 - s_l^{(p)}$
    send $v(m_0{:}m_p)$ to $p + 2^{l-1}$
  elseif $mod\,(p, 2^{l-1}) = 0$ then
    recv $v(m_0{:}m_p)$ from $p - 2^{l-1}$
  endif
enddo

At the end of the procedure, each processor has precisely the coefficients required for the final phase of the coarse grid solve, $\underline{x} = X\underline{c}$. Since the amount of data transmitted at each stage is bounded by the number of ancestors for any given leaf, namely, by the number of nonzeros in any row, we conclude that the total communication complexity for the XX^T algorithm is bounded by $2\log_2 P(\alpha + 3\sqrt{n}\beta)$ for the $\sqrt{n} \times \sqrt{n}$ grid problem.

We comment that we explicitly used a depth-first traversal of the tree (Fig. 2d) in developing the separator-based ordering of the degrees of freedom. Clearly, the same communication complexity is also obtained if one uses a breadth-first traversal. However, the depth-first traversal guarantees that the nonzero pattern within each column of X is contiguous within each processor, as illustrated in Fig. 4d. Consequently, unit-stride direct addressing can be used during the local dot product (7) and DAXPY (9) phases of the $XX^T\underline{b}$ computation, resulting in improved vectorization and cache performance as well as reduced memory overhead.

Finally, we note that the work required to generate X via the Gram-Schmidt procedure (11) is $O(n^2)$ and the time is $O(n^2/P)$. These estimates are derived as follows. Let $W(n)$ be the number of operations required to compute X for a $\sqrt{n} \times \sqrt{n}$ grid. The work required to compute the last $\sqrt{n}$ columns of X is essentially the same as the work required to effect $\sqrt{n}$ projections onto X, namely, $2 \cdot 3n^{\frac{3}{2}}$ operations for each of the dot product and DAXPY phases, yielding an operation count of $12n^{\frac{3}{2}}$ per column. Generation of the $\sqrt{n}/2$ bases associated with each of the two second-level separators (S_1 and S_2) involves projections onto matrices with columns of length $n/2$ and at most $2\sqrt{n}$ nonzeros per row, yielding an operation count bounded by $4n^2$. Generation of the bases associated with all remaining separators comprises four subproblems, each of size $n/4$. Therefore, the total work estimate satisfies the recursion

$$W(n) \quad = \quad 12\,n^2 \;+\; 4\,n^2 \;+\; 4\,W(\frac{n}{4}), \tag{14}$$

The solution to (14) is $W(n) \leq \frac{4}{3}16n^2$. The P-processor time estimate exploits the fact that each of the four subproblems can be treated independently on processor subsets of size

$P/4$. Thus,

$$\begin{aligned} T(n,P) &= 12\,\frac{n^2}{P} + 4\,\frac{n^2}{P} + \frac{4}{4}\,T(\frac{n}{4},\frac{P}{4}) \\ &= 16\,\frac{n^2}{P} + 16\,\frac{n^2}{4^2}\frac{4}{P} + T(\frac{n}{16},\frac{P}{16}) \\ &= 16\,\frac{n^2}{P}\left(1 + \frac{1}{4} + \frac{1}{16} + \ldots\right) \\ &\leq \frac{4}{3}16\,\frac{n^2}{P}\,, \end{aligned} \tag{15}$$

and we conclude that, properly implemented, the Gram-Schmidt procedure attains full P-fold concurrency.

5 Numerical Results

Solution times for the XX^T method on $q \times q$ finite difference meshes for $q = 3, 7, 15, \ldots, 511$ are presented in Table 1. The matrix A (with $n = q^2$) is derived from a 5-point stencil discretization of the Poisson problem with Dirichlet boundary conditions. For comparison we provide corresponding times for both the redundant LU and distributed A^{-1} methods. Note that all times were generated on the 512-node Intel Paragon XPS at Caltech running Paragon OSF/1, release 1.0.4. Also, note that the symbol g in the table indicates a granularity restriction (i.e., $n < P$) while m indicates a memory restriction.

For $P = 1$ or 2, the redundant LU approach is the fastest method in all cases except for the smallest, where the amount of work is insufficient to allow reliable timings. The redundant LU and A^{-1} approach both suffer memory constraints at values of n that are much smaller than achievable with the XX^T approach. For $n \geq 225$, the XX^T approach is the fastest of the three; it is an order of magnitude faster than the A^{-1} approach for $n > 16129$, which is, in turn, an order of magnitude faster than the redundant LU approach.

The table verifies the assertion made in Section 3 that the A^{-1} approach will be superior to the redundant LU approach whenever $P > n/2s$, where s is the matrix bandwidth for the LU scheme. For this problem, $s = \sqrt{n} = q$, implying that the A^{-1} approach should be superior whenever $P > q/2$. The performance transition is observed at precisely this point for all of the entries in the left half of the table. For the larger problems on the right, the transition occurs at lower values of P as the A^{-1} approach benefits from enhanced vector performance as discussed below.

A careful examination of the operation counts for the A^{-1} and XX^T methods reveals that for $n = 3969$ the latter should be ten times faster than the former, instead of the observed fourfold improvement. We found that this result is due to the use of the BLAS library DDOT routine on the Paragon, which, as is seen in Fig. 5c, shows a sudden $2.25\times$ performance gain for vector lengths greater than ≈ 2330. Since the distributed A^{-1} approach requires DDOTs of length n, whereas the XX^T approach requires DDOTs and DAXPYs of at most length n/P or $3\sqrt{n}$, the former method benefits from this vector performance gain, whereas the latter does not for the values of n considered here.

Table 1: Solution time in seconds for a $q \times q$ grid on p processors

p	Red. LU	Dist. A^{-1}	XX^T	Red. LU	Dist. A^{-1}	XX^T
	$n = 3\times3$			$n = 63\times63$		
1	4.4600E-05	3.6105E-05	3.4902E-05	1.1949E-01	–	3.4203E-01
2	1.7068E-04	1.3949E-04	1.3573E-04	1.2003E-01	–	1.9369E-01
4	2.9398E-04	2.5764E-04	2.5064E-04	1.2045E-01	m	8.4266E-02
8	4.6827E-04	3.7863E-04	3.5714E-04	1.2107E-01	1.5573E-01	4.1084E-02
16	g	g	g	1.2186E-01	8.0204E-02	2.0343E-02
32	–	–	–	1.2263E-01	4.2857E-02	1.0608E-02
64	–	–	–	1.2431E-01	2.5133E-02	6.2606E-03
128	–	–	–	1.2692E-01	1.7932E-02	4.1330E-03
256	–	–	–	1.3228E-01	1.7967E-02	3.8113E-03
512	–	–	–	1.4916E-01	2.8438E-02	5.0652E-03
	$n = 7\times7$			$n = 127\times127$		
1	2.9800E-04	3.2989E-04	2.7725E-04	9.1016E-01	–	–
2	4.4168E-04	2.7822E-04	2.9301E-04	9.1129E-01	–	–
4	5.8261E-04	3.4939E-04	3.5085E-04	9.1280E-01	–	m
8	7.4149E-04	4.3863E-04	4.3446E-04	9.1395E-01	–	3.5016E-01
16	9.3307E-04	5.6306E-04	5.7672E-04	9.1594E-01	–	1.6388E-01
32	1.1162E-03	6.9726E-04	7.2160E-04	9.1807E-01	–	8.1527E-02
64	g	g	g	9.1976E-01	m	4.1622E-02
128	–	–	–	9.2159E-01	1.7435E-01	2.2244E-02
256	–	–	–	9.2980E-01	1.2968E-01	1.3643E-02
512	–	–	–	1.0379E+00	1.5087E-01	1.1458E-02
	$n = 15\times15$			$n = 255\times255$		
1	2.0880E-03	9.5215E-03	4.5643E-03	–	–	–
2	2.2781E-03	4.9863E-03	2.3550E-03	–	–	–
4	2.4351E-03	2.7819E-03	1.1259E-03	–	–	–
8	2.6284E-03	1.6877E-03	8.2464E-04	–	–	–
16	2.8119E-03	1.1831E-03	7.9471E-04	–	–	–
32	3.1127E-03	1.0036E-03	9.1089E-04	–	–	m
64	3.2951E-03	1.0952E-03	1.0084E-03	–	–	3.2321E-01
128	3.5418E-03	1.1286E-03	1.1770E-03	–	–	1.6368E-01
256	g	g	g	–	–	8.5836E-02
512	–	–	–	m	m	5.3390E-02
	$n = 31\times31$			$n = 511\times511$		
1	1.6356E-02	1.6719E-01	4.5315E-02	–	–	–
2	1.6640E-02	8.3992E-02	2.1006E-02	–	–	–
4	1.6858E-02	4.2522E-02	9.8550E-03	–	–	–
8	1.7122E-02	2.1893E-02	5.1827E-03	–	–	–
16	1.7501E-02	1.1735E-02	3.0003E-03	–	–	–
32	1.7995E-02	6.8829E-03	2.0195E-03	–	–	–
64	1.8841E-02	4.9585E-03	1.6644E-03	–	–	–
128	1.9221E-02	4.0317E-03	1.5370E-03	–	–	–
256	2.0097E-02	4.0358E-03	1.6672E-03	–	–	m
512	2.1847E-02	5.6248E-03	2.3776E-03	m	m	3.6714E-01

We note that for the $n = 961$, 3969, and 16129 (resp., $q = 31$, 63, and 127) cases the efficiency of all of the methods begins to deteriorate as P approaches 512. These trends are clearly revealed in the plots of solution time vs. number of processors shown in Figs. 5a and b. One would, of course, expect such trends for the fixed-problem-size speedup model; the work scales as $1/P$, while the communication scales as $\log_2 P$. What is surprising is the amount of communication overhead suffered by the A^{-1} approach due to bandwidth constraints. The upward swing at the tails of the curves in Fig. 5a reveal the dominance of communication cost, but the magnitude is well above the latency bound, $\alpha t_a \log_2 P$, which is also plotted. By contrast, the tails of the XX^T curves (Fig. 5b) are much closer to the latency curve, although not as close as might be expected, particularly for the $n = 961$ (31×31) case.

A plot of the total communication overhead for $n \approx P$, added as a dashed line in Fig. 5b, reveals that the XX^T communication costs grow faster than $\log_2 P$ between $P = 256$ and 512. This fact is explained by a design feature of the Paragon operating system, which provides greater bandwidth for smaller numbers of processors, as indicated by the plots of communication time vs. message length shown in Fig. 5d. These times were measured using a standard ping-pong test with noncached data on successive transfers and asynchronous (i.e., preposted) receives for $P = 2$, 4, 8,..., 512. While there is virtually no change in latency as the number of processors increases, there is a fivefold reduction in bandwidth as one moves from $P = 2$ to $P = 512$. This accounts for the faster than $\log_2 P$ growth in communication costs observed in Fig. 5b. Presumably this loss of bandwidth is a result of requiring the system message buffer space to be more finely partitioned in the large P cases. However, in the timings, use of asynchronous receives should have implied that the message buffer memory was managed by the driving application.

Figure 5d also reveals that the linear communication model (3) is adequate at the small and large message limits but does not capture sudden transitions in communication cost which may be significant in actual measured applications. As these nonlinear features are hardware and operating system dependent, there is little one can do to incorporate them into generic complexity estimates in any meaningful way. Actual message-passing performance will always need to be measured to yield a complete understanding of algorithm behavior.

6 Discussion

Because of the generality of the graph-partitioning arguments and the binary tree embeddings employed in developing the XX^T method, the scheme readily extends to general mesh problems. For more complex two- or three-dimensional meshes, separator sets can be found with standard graph-splitting techniques (e.g., recursive coordinate bisection) or via one of the many variants of recursive spectral bisection (e.g., [13]). In general, one can expect somewhat smaller complexity constants than for the examples considered here, as $\sqrt{n}$ is generally the worst-case separator bound for planar graphs. Provided that subdomains are mapped according to the separator induced partitioning, the general geometry implementation of this problem should enjoy the same low communication requirements as the very regular examples considered here.

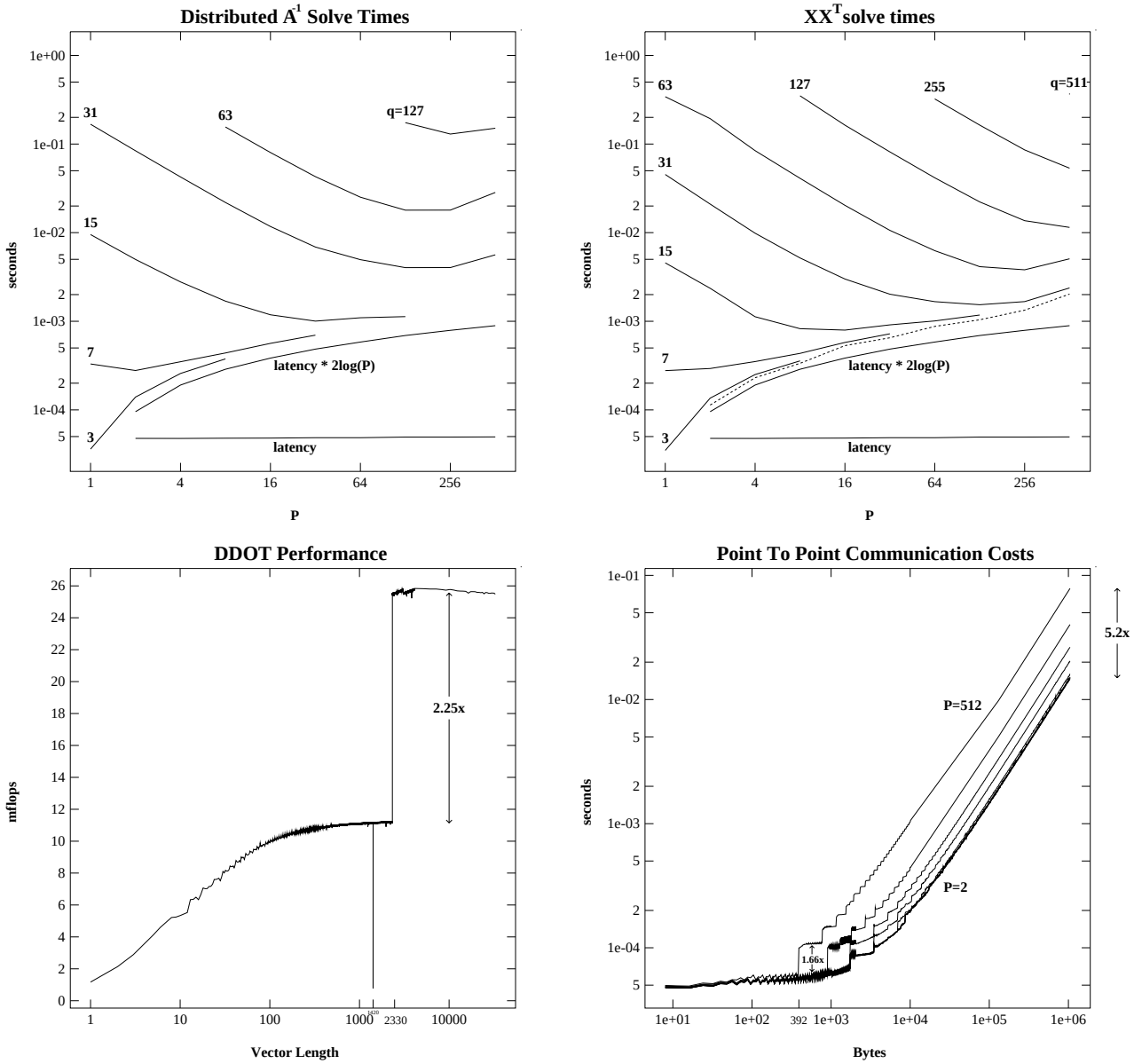

Figure 5: (a) solution times for A^{-1} approach, (b) solution times for XX^T approach, (c) Paragon DDOT performance *vs.* vector length, (d) Paragon communication time *vs.* message size.

In addition, this method can be applied to nonsymmetric problems by solving the problem $A^TA\underline{x} = A^T\underline{b}$. In general, this is inadvisable because of potential ill-conditioning of the system. However, this should not be a problem for the target application of coarse grid problems as these will generally be much better conditioned than the originating larger problem which is being solved iteratively. The foundation for the procedure in the case of a non-symmetric system would be to seek unit vectors $\underline{\hat{e}}_i$, $\underline{\hat{e}}_j$, which are A^TA-conjugate, that is, satisfying $(A\underline{\hat{e}}_i)^TA\underline{\hat{e}}_j = 0$. From considerations similar to those presented in Fig. 1, it is clear that this is achieved by simply choosing separators of width two rather than unity. All of the computational and communication complexity bounds follow immediately in $\mathbb{R}^2$ or $\mathbb{R}^3$, and we expect the nonsymmetric solver to require twice the storage, twice the amount

of data traffic, and precisely the *same* number of messages ($2\log_2 P$) as its symmetric counterpart.

It is possible that further reductions in the number of nonzeros in X may be attained by carefully selecting the generating basis, V, and thresholding small entries in X. This is particularly true in the case where A is being used as a preconditioner, in which case the exact solution to (1) is not required. One promising approach in this regard is to recognize that the computational complexity bounds derived in Section 4 are independent of the choice of basis vectors within a given separator S_l. Therefore, rather than using successive unit vectors, $\underline{\hat{e}}_i$, $i \in S_l$, one might choose a Fourier-like basis having the form

$$\begin{aligned} \underline{v}_i &= \{.....11111111.....\}^T \\ \underline{v}_{i+1} &= \{.....11110000.....\}^T \\ \vdots & \qquad \vdots \\ \underline{v}_{i-1+\#S_l} &= \{.....\underbrace{10101010}_{\text{Support of } S_l}.....\}^T \end{aligned} \tag{16}$$

and which vanish outside the support of S_l. Applied to each separator, this leads to a fill pattern more closely resembling that shown in Fig. 1d rather than a strictly upper-triangular factor. Because the basis vectors $\underline{x}_j$ decay smoothly away from the separators (at least for elliptic problems), the highly oscillatory generating basis should yield columns in X that are effectively zero away from the separator. Initial results for Poisson's equation on a square have shown that the bases (16) do indeed lead to a greater number of "small" entries in X, and to better round-off properties. However, it appears that a smoother set of oscillatory basis functions will ultimately be required if significant savings are to be realized from this thresholding strategy.

Another common strategy for improved performance is to solve the coarse grid problem cooperatively (and redundantly) among processor subsets. The cooperative solve can be implemented with any of the approaches discussed previously, including the XX^T approach. Of course, this does not circumvent the $\log_2 P$ bound on the minimum number of messages and so does little to reduce latency. However, it could be used to ameliorate the nontrivial bandwidth limitations. Our suggested strategy is to gather segments of the right-hand side, $\underline{b}$, onto independent processor subsets using l' rounds of the recursive doubling variant of the Vector Concatenate routine of Section 2. Here, l' is determined such that the message size in the l'th round of the concatenation is equal to a threshold value, m'. For example, let $m' = \min(\alpha/\beta, 3\sqrt{n})$ and choose l' such that $2^{l'-1}n/P = m'$. This ensures that the recursive doubling variant of concatenation does not suffer line contention (since messages shorter than α/β are latency dominated) and does not require message lengths exceeding those required by the XX^T algorithm. After l' rounds of recursive doubling, the coarse grid problem can be solved with the XX^T algorithm using only $2(\log_2 P - l')$ rounds of communication. A similar strategy is employed when $P \neq 2^D$. One identifies the largest value of D such that $P' = 2^D < P$, and maps the right-hand side data from processors $p = P', \ldots, P-1$, onto respective counterparts in $\{0, \ldots, P'-1\}$. The solution is then computed using $P' = 2^D$ processors following the strategy outlined in Section 4.

Finally, we close with predicted performance of the XX^T method on state-of-the-art teraflops machines. Such machines are just coming on line at national DOE laboratories and employ from 3000 to 9000 processors. Our prediction will be based on $P = 8192 = 2^{13}$ processors. We assume that the coarse grid is as small as possible, $n = P$ (the most challenging case), and use the communication constants

$$\begin{aligned} \alpha t_a &= 5.0 \times 10^{-5} \text{ seconds} \\ \beta t_a &= 6.8 \times 10^{-7} \text{ seconds/64} - \text{bit} - \text{word}, \end{aligned}$$

which were derived from the $P = 512$ measurements of Fig. 5d. To estimate the computational cost, we assume a conservative value of $t_a = 1. \times 10^{-7}$ ops/second, corresponding to 10 MFLOPS. For this model problem with $n = P$, the communication cost is

$$\begin{aligned} T_c &= 2\alpha t_a \log_2 P \; + \; 3\sqrt{n}(2\beta + 1)t_a \log_2 P \\ &= 1.3 \times 10^{-3} \; + \; 5.2 \times 10^{-3} \text{seconds}. \end{aligned}$$

The computational cost is

$$\begin{aligned} T_a &= (4 \cdot 3n\sqrt{n}/P)\, t_a \\ &= 0.11 \times 10^{-3} \text{seconds}. \end{aligned}$$

These results reveal that, under reasonable model assumptions, the bandwidth cost (5.2 msec) is of the same order as the latency cost (1.3 msec) and that the arithmetic cost (0.11 msec) is an order of magnitude smaller than the latency cost. Because of the significance of the latency term, it is clear that any competing methods will need to adhere to the strategy of using a minimum number of messages. Moreover, as the bandwidth term is of the same order as the latency term, it becomes more important to focus on reducing the total amount of message traffic than it is to focus on any further reductions in work.

We conclude that the relatively low computational complexity and excellent communication complexity of the XX^T-based solver will make it a very competitive algorithm for leading-edge multicomputer systems. Moreover, since the coarse grid solve is central to efficient iterative solution of many systems arising from partial differential equations, fast coarse grid solvers such as presented here will be critical to future Teraflops applications.

Acknowledgments

This work was supported by the NSF under Grant ASC-9405403 and by the AFOSR under Grant F49620-95-1-0074. Computer time was provided on the Intel Paragon and Delta at Caltech under NSF Cooperative agreement CCR-8809615 and on the Intel Paragon at Wright Patterson Air Force Base by the AFOSR.

References

[1] F. Alvarado, A. Pothen, and R. Schreiber, "Highly parallel sparse triangular solution", Univ. Waterloo Research Rep. CS-92-51, Waterloo, Ontario, 1992.

[2] X.-C. Cai, "The use of pointwise interpolation in domain decomposition with non-nested meshes," *SIAM J. Sci. Comput.*, **14** (1995) pp. 250–256.

[3] T. Chan and J. P. Shao, "Parallel complexity of domain decomposition methods and optimal coarse grid size", *Parallel Computing*, **21** (1995) pp. 1033–1049.

[4] M. Dryja and O. Widlund, "Towards a unified theory of domain decomposition algorithms for elliptic problems", in *Proceedings of the Third International Symposium on Domain Decomposition Methods for Partial Differential Equations*, R. Glowinski, J. Periaux, and O. Widlund, eds., SIAM, Philadelphia, p. 3, 1990.

[5] C. Farhat and P. S. Chen, "Tailoring domain decomposition methods for efficient parallel coarse grid solution and for systems with many right hand sides," *Contemporary Math.*, **180** (1994) p. 401–406 .

[6] P. F. Fischer, "Parallel domain decomposition for incompressible fluid dynamics", *Contemporary Mathematics*, **157** (1994) pp. 313–322.

[7] P. F. Fischer, "Parallel multi-level solvers for spectral element methods", in *Proceedings of Intl. Conf. on Spectral and High-Order Methods '95, Houston*, *Houston J. Math.*, R. Scott, ed., (1996) pp. 595–604.

[8] J. A. George, "Nested dissection of a regular finite element mesh", *SIAM J. Numer. Anal.*, **15** (1978) pp. 1053–1069.

[9] W. D. Gropp, "Parallel computing and domain decomposition", in *Fifth Conference on Domain Decomposition Methods for Partial Differential Equations*, T. F. Chan, D. E. Keyes, G. A. Meurant, J. S. Scroggs, and R. G. Voigt, eds., SIAM, Philadelphia, 1992.

[10] W. D. Gropp and D. E. Keyes, "Domain decomposition with local mesh refinement", *SIAM J. Sci. Stat. Comput.*, **15** 4 (July 1992) pp. 967–993.

[11] D. E. Keyes, Y. Saad, and D. G. Truhlar, *Domain-Based Parallelism and Problem Decomposition Methods in Computational Science and Engineering*, SIAM, 1995.

[12] J. L. Gustafson, G. R. Montry, and R. E. Benner, "Development of parallel methods for a 1024-processor hypercube", *SIAM J. on Sci. and Stat. Comput.*, **9** 4 (1988) p. 609.

[13] A. Pothen, H. D. Simon, and K. P. Liou, "Partitioning sparse matrices with eigenvectors of graphs", *SIAM J. Matrix Anal. Appl.*, **11** 3 (1990) pp. 430–452.

[14] B. Smith, P. Bjørstad, and W. Gropp, *Domain Decomposition*, Cambridge University Press, 1996.

[15] R. van de Geijn, "On global combine operations," *J. Parallel & Distributed Comput.*, **22** (1994) pp. 324–328.

[16] O. B. Widlund, "Iterative substructuring methods: Algorithms and theory for elliptic problems in the plane", in *Proceedings of the First International Symposium on Domain Decomposition Methods for Partial Differential Equations*, R. Glowinski, G. H. Golub, G. A. Meurant, and J. Periaux, eds., SIAM, Philadelphia, 1988.